High field magnetic transitions in the mixed holmium–yttrium iron garnet $Ho_{0.43}Y_{2.57}Fe_5O_{12}$

2005 J. Phys.: Condens. Matter 17 241

(http://iopscience.iop.org/0953-8984/17/1/023)

INSTITUTE OF PHYSICS PUBLISHING JOURNAL OF PHYSICS: CONDENSED MATTER

J. Phys.: Condens. Matter **17** (2005) 241–248 doi:10.1088/0953-8984/17/1/023

High field magnetic transitions in the mixed holmium–yttrium iron garnet $Ho_{0.43}Y_{2.57}Fe_5O_{12}$

A Bouguerra[1,2], S Khène[3], S de Brion[4], G Chouteau[4] and G Fillion[1,5]

[1] Laboratoire Louis Néel, CNRS, BP166, F-38042 Grenoble cedex 9, France
[2] ISET, Centre Universitaire de Tebessa, 12002 Tebessa, Algeria
[3] Département de Physique, Université d'Annaba, BP-12, 23000 Annaba, Algeria
[4] Grenoble High Magnetic Field Laboratory, CNRS and MPI-FKF, BP166, F-38042 Grenoble cedex 9, France

E-mail: fillion@grenoble.cnrs.fr

Received 18 September 2004, in final form 16 November 2004
Published 10 December 2004
Online at stacks.iop.org/JPhysCM/17/241

Abstract

High static magnetic field magnetization measurements have been performed up to 23 T on $Ho_{0.43}Y_{2.57}Fe_5O_{12}$ single crystals at helium temperature ($T = 4.2$ K) with fields applied along the three main cubic axes: $\langle 111 \rangle$, $\langle 110 \rangle$ and $\langle 001 \rangle$. The change from the spontaneous ferrimagnetic structure in zero magnetic field to the fully ferromagnetic one in high field takes place through several intermediate phases separated by transitions with step-like magnetization behaviour, but without any observed hysteresis. Using the effective spin Hamiltonian approximation, we show that the general features of these transitions can be accounted for by a large magnetocristalline anisotropy of the Ho^{3+} moments of the uniaxial type along the local z axis of each rare-earth site. The model is in better agreement with the experiments than its Ising limit, widely used before, but is still unsuccessful in predicting the 'umbrella' magnetic structures found by previous neutron and NMR experiments.

(Some figures in this article are in colour only in the electronic version)

1. Introduction

In the ferrimagnetic holmium–yttrium iron garnet, as in all the rare-earth iron garnets (RIGs), the iron intrasublattice exchange interactions (∼200 T) far exceed the iron–rare-earth intersublattice interactions (∼10–20 T), which, in turn, exceed the rare-earth intrasublattice interactions (∼1 T). Therefore, in the available dc fields, the Ho^{3+} cations on the 24c site play the role of a weak or 'captive' sublattice, whereas the net 'a–d sublattice' of the Fe^{3+} cations, on the 16a and 24d sites, acts as one 'strong' sublattice with a moment $M_{Fe} = M_d - M_a$.

[5] Author to whom any correspondence should be addressed.

Whereas the Fe^{3+} anisotropy can be neglected, the Ho^{3+} anisotropy is actually very important at low temperature, and the direction and magnitude of the holmium moments result mainly from the interplay of (i) their large local anisotropy, (ii) the holmium–iron exchange interaction and (iii) the external field action. For the six rare-earth sublattices, inequivalent with regard to their local environment, this leads to the formation of conical arrangements of their moments (the so-called 'umbrella' structures [1–3]) around one of the $\langle 111 \rangle$ axes, which are the overall easy axes for most of the RIGs and especially for the studied $Ho_{0.43}Y_{2.57}Fe_5O_{12}$ compound. In this material, the net moment M_{Ho} of all the holmium sublattices is always smaller than the iron one and antiparallel to it in zero field, and so there is no compensation point in this compound.

Previous experiments on related compounds in pulsed fields [4–7] or in static fields [8] have shown that, at sufficiently low temperature, the increase of the applied field H gives rise to 'orientational' phase transitions with step-like magnetization curves, corresponding to the passage from the initial ferrimagnetic state to the ferromagnetic saturated state through several canted phases. The number of these transitions depends on the orientation of the external field with respect to the crystallographic axes. At higher temperatures, the rare earth anisotropy is less effective and the reversal of the Ho moments is achieved first by demagnetization, then by passing through zero values when H cancels the mean iron exchange field, and finally by remagnetization up to saturation [9]. As a first explanation, it was previously assumed [10, 5–7] that each Ho^{3+} magnetic moment had such huge anisotropy that it is rigidly fixed to its local surrounding z axis. Under the action of the effective iron exchange field and the external field, the six Ho sublattices are reduced to only three with their moments equal and parallel to each $\langle 001 \rangle$ cell fourfold axis. The resultant Ho moment M_{Ho} then lies along one of the eight $\langle 111 \rangle$ directions and this leads us to consider a maximum number of eight possible domains or phases. The magnetization jumps are then ascribed to the discrete passage of M_{Ho} from one $\langle 111 \rangle$ direction to another, as a result of the successive reversal of the moments of the different Ho sublattices. During these reversals, the direction of the iron moment M_{Fe} changes into its new equilibrium position. For peculiar directions $\boldsymbol{u}$ of the applied field H, several of these $\langle 111 \rangle$ domains can have the same projection on H, and so they are equivalent and belong to the same degenerate phase. The number $n_p(\boldsymbol{u})$ of inequivalent phases ($P^i_{\boldsymbol{u}}$, $i = 1$ to n_p) is then reduced together with the number of observable magnetization steps ($n_p(\boldsymbol{u}) - 1$), especially if the applied field H is oriented along high symmetry directions. For H along [111], the four phases are $P^1_{111} = \{[\bar{1}\bar{1}\bar{1}]\}$, $P^2_{111} = \{[1\bar{1}\bar{1}], [\bar{1}1\bar{1}], [\bar{1}\bar{1}1]\}$, $P^3_{111} = \{[11\bar{1}], [\bar{1}11], [1\bar{1}1]\}$ and $P^4_{111} = \{[111]\}$, giving rise to three transitions between them when the applied field successively reverses the moments of Ho sublattices from the configuration with the resultant moment $M_{Ho} \parallel [\bar{1}\bar{1}\bar{1}]$ to the saturated one with $M_{Ho} \parallel [111]$. On the same manner, for $H \parallel [110]$, there are two transitions between the three phases $P^1_{110} = \{[\bar{1}\bar{1}\bar{1}], [\bar{1}\bar{1}1]\}$, $P^2_{110} = \{[1\bar{1}\bar{1}], [\bar{1}1\bar{1}], [1\bar{1}1], [\bar{1}11]\}$ and $P^3_{110} = \{[11\bar{1}], [111]\}$. For $H \parallel [001]$, only one jump can occur between the two phases $P^1_{001} = \{[\bar{1}\bar{1}\bar{1}], [1\bar{1}\bar{1}], [\bar{1}1\bar{1}], [11\bar{1}]\}$ and $P^2_{001} = \{[\bar{1}\bar{1}1], [1\bar{1}1], [\bar{1}11], [111]\}$.

In order to examine in more detail this quasi-Ising model and to improve the determination of the involved parameters, we have undertaken precise magnetization measurements of these transitions in $Ho_{0.43}Y_{2.57}Fe_5O_{12}$ single crystals under high static magnetic fields up to 23 T. In this paper we are reporting the results obtained at liquid helium temperature with the field oriented along the three main crystallographic axes: $\langle 111 \rangle$, $\langle 110 \rangle$ and $\langle 001 \rangle$. Theoretical magnetization curves are calculated within the framework of the effective spin Hamiltonian approximation [11]. They are compared with the experimental ones and their physical implications are discussed.

2. Experimental details and results

Several single crystals of $Ho_xY_{3-x}Fe_5O_{12}$ with a nominal holmium concentration $x = 0.4$ have been grown by the standard PbO/PbF_2 flux method [12]. Two sets of samples have been cut in an almost spherical shape of about 5 mm (size 1) and 3 mm (size 2) in diameter respectively, corresponding to an average of 0.3 and 0.06 g. They have been oriented along the main cubic axes ⟨001⟩, ⟨110⟩ and ⟨111⟩ by the common x-ray Laüe technique and encapsulated in special sample holders, filled with a methacrylate resin [13] in order to keep them well fixed even with the huge torque developed under high field. The total misalignment with the applied field H in all the experiments is estimated to be less than 2° in angle. The chemical composition was checked using a scanning microscope (JSM-840A), electronic microprobe and chemical analysis and also by checking carefully the specific magnetization of each sample in the low field range. The results of these different methods show a greater dispersion than for the previously studied compound ($x = 0.24 \pm 0.01$) [8] and the composition was found to vary from $x = 0.41$ to 0.45. So we take $x = 0.43 \pm 0.02$, and all the magnetization results are reported in Bohr magnetons per $Ho_{0.43}Y_{2.57}Fe_5O_{12}$ formula unit.

The magnetization value has been recorded using an extraction technique either in the two superconducting magnets of the Laboratoire Louis Néel (LLN) up to 10 and 16 T for sample size 1 & 2, or in the 23 T water cooled magnet of the Grenoble High Magnetic Field Laboratory (GHMFL) for sample size 2 only. The measurements were made at a rate of about one per minute. For the calibration of the different experiments, the same spherical single crystal of YIG was used, the magnetization of which was carefully checked to be 5.016 μ_B/fu $Y_3Fe_5O_{12}$ at 2 K in the easy ⟨111⟩ direction.

The magnetization curves, obtained at the liquid helium temperature $T = 4.2$ K, when the magnetic field H is applied along the different main crystallographic axes, are shown in figures 1(a), (b) and (c) respectively. They bring to evidence rather sharp steps in magnetization as the H strength is increased to the maximum and then decreased to zero. Their number for each direction is as expected: three for $H \parallel \langle 111 \rangle$, two for $H \parallel \langle 110 \rangle$ and one for $H \parallel \langle 001 \rangle$.

It is worth noting that, within the relative experimental errors, all the observed transitions are free of hysteresis, and that when the applied field is along the easy axis of magnetization ⟨111⟩ the absolute saturation is quickly achieved after the last jump (figure 1(c)).

The value of the spontaneous magnetization is $M_o(\boldsymbol{H} \parallel \langle 111 \rangle) = 2.07 \pm 0.09\ \mu_B$/fu. Taking the magnetization of the iron sublattice as the experimental value for YIG, $M_{Fe} \cong M_{YIG} = 5.02\ \mu_B$/fu, it corresponds to $M_{Ho} = 2.95 \pm 0.09\ \mu_B$/fu and a mean Ho^{3+} moment of $6.86 \pm 0.21\ \mu_B$ projected along the ⟨111⟩ easy axis.

3. Discussion

The numerical magnetization curves are obtained as in our previous paper [8] by using the framework of the effective spin Hamiltonian model (ESH) [11]: The free energy F of one molecule of $Ho_xY_{3-x}Fe_5O_{12}$ is

$$F = -\boldsymbol{M}_{Fe}\mu_0\boldsymbol{H} - \frac{x}{6}k_BT\sum_{q=1}^{6}\ln 2\mathrm{ch}\left(\frac{\Delta_q}{k_BT}\right) \qquad \text{where } \Delta_q = \left|-\mu_B\mu_0\boldsymbol{H}\tilde{\boldsymbol{g}}_q + \frac{\boldsymbol{M}_{Fe}}{M_{Fe}}\tilde{\boldsymbol{G}}_q\right|,$$

$\tilde{\boldsymbol{g}}$ is the paramagnetic tensor, $\tilde{\boldsymbol{G}}_q = \mu_B M_{Fe}\tilde{\boldsymbol{n}}\tilde{\boldsymbol{g}}_q$ is the exchange tensor, $\tilde{\boldsymbol{n}}$ is the molecular field coefficient tensor and the sum is over the six inequivalent holmium sites of D_2 symmetry. This model has the advantage of including the quasi-Ising model corresponding to the case of finite g_z and null values for g_x and g_y for the $\boldsymbol{g}$ tensor diagonal parameters, which is

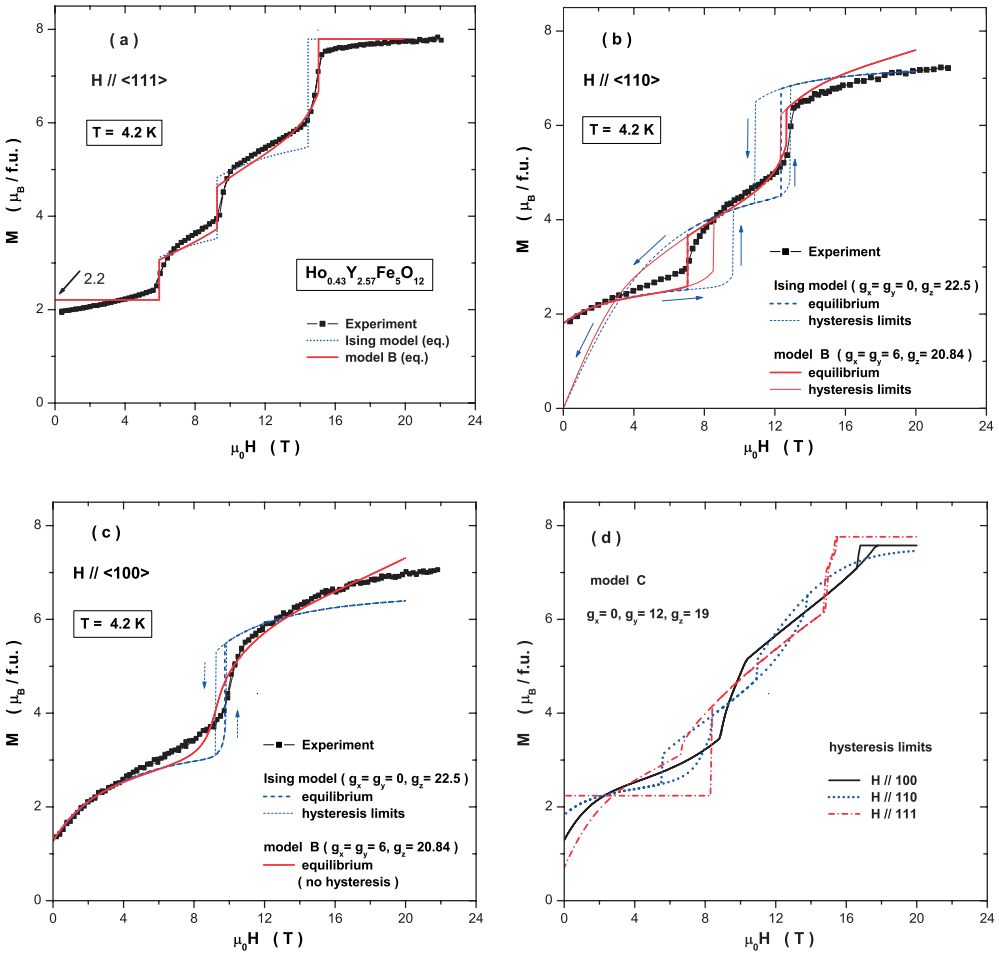

Figure 1. Magnetization curves of $Ho_{0.43}Y_{2.57}Fe_5O_{12}$: (a) $H \parallel \langle 111 \rangle$, (b) $H \parallel \langle 110 \rangle$, (c) $H \parallel \langle 001 \rangle$, (d) model C.

referred to in the following as the Ising model or model A. With given values for the $\boldsymbol{g}$ tensor, the field $\boldsymbol{H}$ and the temperature T, the net holmium moment $\boldsymbol{M}_{\mathrm{Ho}}$ and the free energy F of the system $Ho_{0.43}Y_{2.57}Fe_5O_{12}$ are calculated with respect to the two polar angles θ and ϕ of the iron sublattice magnetization vector $\boldsymbol{M}_{\mathrm{Fe}}$, using the Scilab environment [14] on a PC computer. All the minima of this energy surface $F(\theta, \phi)$ can then be easily located and well determined by a quasi-Newton method, not only the lowest one corresponding to the ground state, but also the other local minima which are related to metastable states. For each couple (θ, ϕ), the configuration of the moments is fully determined and the phases can be assigned to each minimum without any ambiguity. When the $M(H)$ curves are calculated, if the lowest energy minimum is always taken for each value of the field $\boldsymbol{H}$, the curves are reversible, i.e. independent of the sample field history, and they correspond to thermodynamical equilibrium and true isothermal conditions. But one can also follow by continuity the metastable states until their limit of stability, when they become unstable as the determinant of the F second order local derivatives vanishes. The $M(H)$ curves obtained in this way show the maximum possible hysteresis when H is increased or decreased in a continuous way.

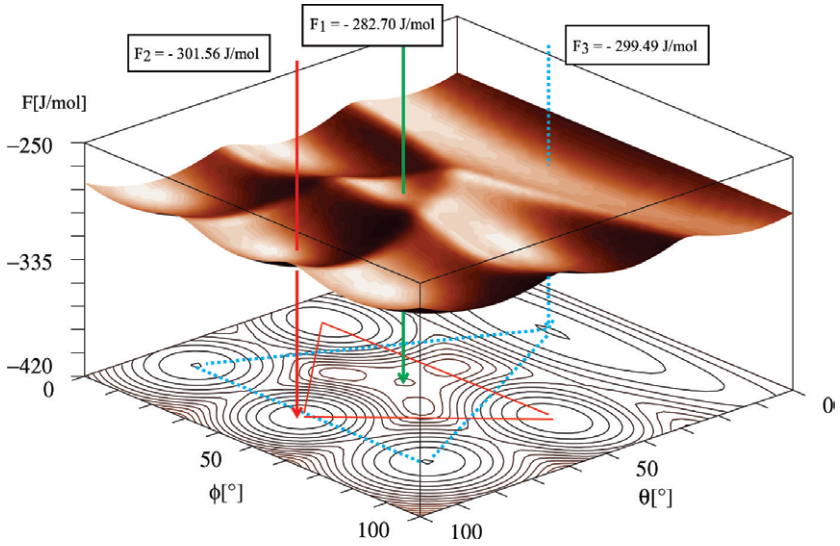

Figure 2. Free energy surface $F(\theta, \phi)$ and its contour plot for the Ising model (ESH with $g_x = g_y = 0$, $g_z = 22.5$), with $\boldsymbol{H} = 9$ T $\parallel$ [111] at $T = 4.2$ K; θ and ϕ are the polar angles of the magnetization vector $\boldsymbol{M}_{Fe}$ in degrees. The projections of the minima with the same energy $F2$ or $F3$ are connected respectively by solid and dashed lines. The energy interval between two successive contour lines is 2 J mol^{-1}.

This is illustrated as an example in figure 2, where the energy surface $F(\theta, \phi)$ is shown for $\mu_0 \boldsymbol{H} = 9$ T $\parallel$ [111], just below the second transition in the Ising case (see also figure 1(a)). In order to not introduce more variables, the same values as in [8], except $x = 0.43$, have been taken for the other parameters: $M_{Fe} = 5\ \mu_B$/fu, $g_x = g_y = 0$, $g_z = 22.5$ and an isotropic effective exchange field $\mu_0 H_{exch} = 11$ T which correspond to an isotropic molecular exchange coefficient tensor $n = 2.2$ T mol/μ_B and a field of 26.5 T acting on the true spin $\boldsymbol{S}$. In these conditions, the initial phase P^1_{111} of free energy F1 with $\boldsymbol{M}_{Ho} \parallel [\bar{1}\bar{1}\bar{1}]$ and $\boldsymbol{M}_{Fe} \parallel \boldsymbol{H} \parallel [111]$ is no longer the ground state after the first transition at $\mu_0 H_{c1} = 5.95$ T, but remains metastable until 9.6 T. The second phase P^2_{111} corresponds to the three minima around [111] with the same lowest free energy $F2 = -301.56$ J mol^{-1} (=36.27 K) and $\boldsymbol{M}_{Ho}$ along one of the directions $[1\bar{1}\bar{1}]$, $[\bar{1}1\bar{1}]$ or $[\bar{1}\bar{1}1]$. The three other minima of energy $F3 = -299.49$ J mol^{-1} (=36.02 K) correspond to the third phase P^3_{111} with $\boldsymbol{M}_{Ho} \parallel [11\bar{1}]$, $[\bar{1}11]$ and $[1\bar{1}1]$ respectively. They will become the lowest ones for $\mu_0 H > \mu_0 H_{c2} = 9.25$ T. The final saturated phase P^4_{111} in high fields ($\boldsymbol{M}_{Ho} \parallel \boldsymbol{M}_{Fe} \parallel \boldsymbol{H} \parallel [111]$) is not stable before 12.8 T but becomes the ground state for $\mu_0 H > \mu_0 H_{c3} = 14.45$ T.

It can also be seen in figure 2 that the lowest energy barrier between the two phases P^2_{111} ($F2$) and P^3_{111} ($F3$) is about 10 J mol^{-1}, a few more than 1 K. It is therefore quite normal that no hysteresis can be observed in our experiments, performed at 4.2 K or even 1.7 K, and we would need to lower the temperature down to the millikelvin range in order to see this signature of the first order nature of the transitions. The hysteresis observed in the previous pulsed field experiments is most probably due to the high level of field sweeping rate, together with magnetocaloric effects and thermodynamics inside the sample, and, as an added remark, the critical fields are systematically higher in pulsed fields than in our static measurements.

The curves at equilibrium are reported in figures 1(a)–(c) for each applied field direction, together with the stability limits and the corresponding curves, except in figure 1(a), where

Table 1. Transition critical fields for the different directions of the applied magnetic field.

Applied field direction	⟨111⟩			⟨110⟩		⟨001⟩	
Critical field (T)	$\mu_0 H_{c_1}$	$\mu_0 H_{c_2}$	$\mu_0 H_{c_3}$	$\mu_0 H_{c_1}$	$\mu_0 H_{c_2}$	$\mu_0 H_{c_1}$	$\mu_0 H_{c_2}$
Pulsed fields[a]	9.0	12.2	16.2	8.5	13.9	12.2	
	8.1	10.6	15.8	7.5	13.1	11.3	n.a.
Static fields (this work)	**6.0**	**9.5**	**14.9**	**7.2**	**12.9**	**10.0**	>22
Ising (model A)[b]	9.6	11.7	15.1	9.6	12.9	9.8	
	5.95[e]	9.25	14.45	7.05	12.35	9.75	
	0	0	12.8	0	10.9	9.2	n.a.
Model B[c]	9.0	11.0	15.2	8.5	12.7		
	5.95	9.25	15.05	7.05	12.65	9.2	
	0	0	14.3	0	12.3		n.a.
Model C[d]	8.35	14.9	15.5	8.35	10.95–13.75	8.85–10.35	17.8
	0	14.7	15.3	5.55			16.7

[a] See [5].
[b] ESH with $g_x = g_y = 0$, $g_z = 22.5$.
[c] $g_x = g_y = 6$, $g_z = 20.84$.
[d] $g_x = 0$, $g_y = 12$, $g_z = 19$.
[e] Calculated values at equilibrium are underlined.

the very large calculated hysteresis for each phase would lead to an intricate and confusing situation. The different critical fields which can be estimated are also reported in table 1.

The calculated values at thermodynamical equilibrium for the Ising model are surprisingly in fair agreement with our observations, but the magnetization jumps are overestimated, and the slope between the transitions is too small (figure 1). Further, as already pointed out [15], the g_z value of 22.5, which gives a spontaneous overall moment in agreement with the experiment, is too high because the calculated Ho moment is then 11.25 μ_B, well above the maximum free ion value of 10 μ_B.

In order to avoid this problem and to improve the model, we have tried in model B to keep for Ho a large but not infinite anisotropy of the uniaxial type around the z local axis, taking $g_x = g_y = 6$ and $g_z = 20.84$ as an example, with a corresponding Ho moment of 9.7 μ_B. The critical fields are about the same or even better, with less hysteresis. The magnetization jumps are also in better agreement, especially for the upper ones in figures 1(a) and (b) for the ⟨111⟩ and ⟨110⟩ directions respectively. For the ⟨001⟩ case, figure 1(c), the general shape of the magnetization curve is closer to the experimental one and the nature of the calculated transition has changed to second order with no calculated hysteresis. These improvements seem to confirm the uniaxial nature of the local Ho anisotropy. Nevertheless, the two precedent models give rise to only one magnetic structure of the Ho moments around ⟨111⟩ in the spontaneous groundstate, while it has been observed by neutron diffraction and NMR techniques that there are two different 'umbrellas', one with a moment $m_1 \sim 9.5\ \mu_B$ close to the maximum free ion value and a small cone angle $\psi_1 \sim 18°$–$33°$, the other with a smaller moment $m_2 \sim 8\ \mu_B$ but a greater conical angle $\psi_2 \sim 50°$–$60°$ close to the local z axis angle [1–3]. In the frame of the SEH model and the isotropic molecular exchange hypothesis, there are only two ways to obtain such different 'umbrellas', one is for $g_x/g_z \sim 0$ and $g_y/g_z \sim 0.6$, and the other for $g_x/g_z \sim 0.6$ and $g_y/g_z \geqslant 1$. The last one has to be rejected because in that case the easy direction for M_{Fe} is no longer the threefold axis ⟨111⟩ but has become the fourfold axis ⟨001⟩.

So we tried a calculation (model C) with the values of the $\boldsymbol{g}$ tensor $g_x = 0$, $g_y = 12$ and $g_z = 19$, which give $m_1 = 9.5\ \mu_B$, $\psi_1 = 54.7°$, $m_2 = 8.1\ \mu_B$ and $\psi_2 = 25.3°$. The results are shown in figure 1(d) and it is obvious that they are in poor agreement with the experiments, especially for the $\langle 111 \rangle$ and the $\langle 001 \rangle$ directions, where for the former the second and third transitions are pushed close together in high fields with very little hysteresis, and for the latter by the appearance of a second first order transition to saturation and a continuum of second order transitions in the middle.

This seems to show that the magnetization behaviour under high magnetic fields and the magnetic structures found by neutron and NMR experiments are somewhat inconsistent or that the ESH model is unable to account for this system. Some improvements can be made by introducing a large exchange anisotropy but it would add at least two other parameters for the $\boldsymbol{G}$ tensor and then any fit would have little chance to be reliable.

The most questionable hypothesis which is underlying in the ESH model is that the crystal field energy levels are changing linearly under the Zeeman effect of the external magnetic field or the effective exchange field. As has been already remarked [15], this may be not the case for the Ho^{3+} ions especially as, due to the peculiar arrangement of the magnetic structure, the magnitude of the total acting field is decreased from about 10 T to almost zero and then increased again to about the same or higher values when the external field is varied upwards. The model is then valid only for a reduced window of field and, in other words, is not suitable in the whole range of fields with the same values of the parameters. Nevertheless, a direct crystal field calculation, including external magnetic field and exchange interaction effects, would involve even more parameters and need very reliable constraints.

4. Conclusion

We have made a precise determination of the spin reorientation transitions under high magnetic fields on the $Ho_{0.43}Y_{2.57}Fe_5O_{12}$ compound. The comparison with the calculations in the effective spin Hamiltonian approximation (ESH models B and C) shows that the nature of the transitions, especially for the high field ones, the associated magnetization jumps and the slope between them are very sensitive to the $\boldsymbol{g}$ tensor parameters, but in contrast the critical fields are less affected. An attempt to account for the double-'umbrella' structure with an isotropic molecular exchange field (model C) was unsuccessful, and this led us to consider a large anisotropy of the Ho–Fe exchange interactions either in the ESH model, with parameters depending on H, or in a direct crystal field calculation. But, first, because of the greater number of involved parameters, the constraints to the fit have to be more carefully checked.

Acknowledgments

We warmly thank Dr A Markosyan for providing us with the samples, Professor A Zvezdin for helpful discussions and A Richard for technical assistance during the high field experiments. The Grenoble High Magnetic Field Laboratory is 'laboratoire associé à l'Université Joseph Fourier—Grenoble'. AB acknowledges the support of the French–Algerian training grant programme BFA no 2002652.

References

[1] Herpin A, Koehler W and Meriel P 1960 *C. R. Acad. Sci. Paris* **251** 1350
[2] Guillot M, Tchéou F, Marchand A and Feldmann P 1984 *Z. Phys.* B **56** 29
[3] Englich J, Lütgemeier H, Pieper M W, Nekvasil V and Novák P 1985 *Solid State Commun.* **56** 825

[4] Demidov V G and Levitin R Z 1977 *Sov. Phys.—JETP* **45** 581
[5] Silant'ev V I, Popov A I, Levitin R Z and Zvezdin A K 1980 *Sov. Phys.—JETP* **51** 323
[6] Babushkin G A, Zvezdin A K, Levitin R Z, Popov A I and Silant'ev V I 1981 *Sov. Phys.—JETP* **53** 1015
[7] Lagutin A S 1994 *Physica* B **201** 63
[8] Bouguerra A, Khène S and Fillion G 2004 *Phys. Status Solidi* c **1** 1683
[9] Levitin R Z, Ponomarev B K and Popov Yu F 1971 *Sov. Phys.—JETP* **32** 1056
[10] Zvezdin A K, Mukhin A A and Popov A I 1977 *Sov. Phys.—JETP* **45** 573
[11] Alben R 1970 *Phys. Rev.* B **2** 2767 and references therein
[12] Gapeev A K, Levitin R Z, Markosyan A S, Mill' B V and Perakalina T M 1975 *Sov. Phys.—JETP* **40** 117
[13] Mecaprex KM-U *Société PRESI, Brie et Angonnes, 38320 Grenoble, France*
[14] Gomez C (ed) (INRIA—Rocquencourt, France) 1999 *Engineering and Scientific Computing with Scilab* (Boston, MA: Birkhaüser) ISBN: 0-8176-4009-6
[15] Lagutin A S 1992 *Sov. Phys.—JETP* **75** 138